JOURNAL OF AGRICULTURAL AND FOOD CHEMISTRY

Structure, Chemical Composition, and Xylanase Degradation of External Layers Isolated from Developing Wheat Grain

JOHNNY BEAUGRAND,† DAVID CRÔNIER,† PASCAL THIEBEAU,§ LUCAS SCHREIBER,# PHILIPPE DEBEIRE,† AND BRIGITTE CHABBERT*,†

Equipe Parois Végétales et Matériaux Fibreux, UMR FARE-614, and Unité d'Agronomie Laon-Reims-Mons, Institut National de la Recherche Agronomique, 2 Esplanade Roland Garros, 51686 Reims Cedex 02, France; and Ecophysiology of Plants, Institute of Cellular and Molecular Botany (IZMB), University of Bonn, Kirschallee 1, D-53115 Bonn, Germany

The external layers of wheat grain were investigated during maturation with respect to chemical and structural features and xylanase degradability. Cytochemical changes were observed in the isolated peripheral tissues of the wheat grain at four defined stages following anthesis. Marked chemical changes were highlighted at 11 days after anthesis, for which protein and lipid contents varied weakly. The profile of esterified ferulic acid showed large variation in the maturing peripheral layers of grain in contrast to the deposition of ferulate dimers, *p*-coumaric and sinapic acids. Lignin was monitored at the latest stages of ripening, which corresponds to the cessation of reserve accumulation in the grain. Arabinoxylans (AX) reached a maximum at 20 days and did not display any significant change in arabinosyl substitution proportion until ripeness. When submitted to xylanase, all outer layers were similarly altered in the proportion of soluble AX except for the peripheral tissues of the 11-day-aged wheat grain that had very little AX. Aleurone and nucellar layers were mostly degraded, whereas pericarp stayed intact at all stages of maturation. This degradation pattern was connected with the preferential immunolocalization of xylanase in aleurone and nucellar layers irrespective of the developmental stages. Further chemical examination of the enzyme-digested peripheral tissues of the grain supports the facts that ferulic ester is not a limiting factor in enzyme efficiency. Arabinose branching, ferulic dimers, and ether-linked monomers that are deposited early in the external layers would have more relevance to the in situ degradability of AX.

KEYWORDS: Peripheral tissues of the wheat grain (*Triticum aestivum*); maturation; cell wall; arabinoxylans; xylanase; immunolocalization; phenolic acids; lignin; aleurone; cutin, alkylresorcinol

INTRODUCTION

Wheat bran is a hemicellulose-rich milling product that may be processed in addition to its main use in animal feeding. Wheat bran thus constitutes an industrial product obtained from grain dry-milling and represents a heterogeneous laminate of several kinds of cells having distinct botanical origins and structural compositions. These layers are the peripheral tissues of the grain including, from the inside to the outside, the aleurone layer (al), the nucellar lysate, the nucellar layer (nl) (*1*, *2*), the testa (t), and the pericarp (*3*, *4*). Both the nl and t have a cuticle of lipophilic material (*5*). Pericarp consists of tube cells (tc), cross cells (cc), hypodermis, and finally the epidermis. Wheat bran thus mainly consists of cell walls but also contains noticeable amounts of micronutrients such as vitamins and phytosterols, mainly due to presence of the aleurone (*4*, *6*).

Considering the great importance of cereal in human nutrition, some basic knowledge has been provided regarding arabinoxylans (AX) in the scope of cereal processing that aims at food and nonfood uses (*7*). Indeed, arabinoxylans are the main hemicelluloses encountered in wheat brans and account for ∼40% of the dry matter of destarched wheat bran (*8*). More specifically, wheat bran AX consist of a (1→4)-β-D xylopyranose backbone and have substitution side chains including α-L-arabinofuranose groups and to a much lower extent glucuronic acid or its methyl derivative and acetyl groups. Phenolic acids are the main interconnecting agents between polymers in graminaceous cell walls. Ferulic acid (FA) is reported to mainly cross-link polysaccharides, whereas *p*-coumaric acid (pCA) would also cross-link lignin (*9*−*15*). Ferulic acid and its dehydrodimer forms (DHD) both link to the *O*-5 arabinofuranosyl residue and are the major phenolic acids in bran cell walls (*10*). pCA and sinapic acid (SA) are found in much lower amounts. The potential role of structural protein in cross-linking AX was recently highlighted (*16*). Other wall components, such as β-glucan and cellulose, may also interact with AX through

* Corresponding author (tel 33 3 26773597; fax 33 3 267753599; e-mail chabbert@reims.inra.fr).
† Equipe Parois Végétales et Matériaux Fibreux, INRA.
§ Unité d'Agronomie Laon-Reims-Mons, INRA.
# University of Bonn.

10.1021/jf049529w CCC: $27.50
Published on Web 10/19/2004

non-covalent interactions (*17*). The resulting cohesive wall network provides the grain with a strong mechanical and biological resistance. Likewise, xylanase degradation of wheat brans was shown to be tissue-specific; meanwhile, the outermost bran layers were enzyme-recalcitrant despite their low lignin contents (*18*).

The present investigation aimed at evaluating the impact of outer-layer changes across grain ripening on the in situ degradation of the AX of the grain peripheral tissues with a (1→4)-β-endo-xylanase (EC 3.2.1.8) from family 11 of the glycoside hydrolase classification system, commonly named family 11 xylanase. This enzyme cleaves the internal β-1,4-xylosidic linkages in the xylan backbone. Considering the maturation of wheat grains, little information is available on the chemical aspects of the external layers when compared to the whole grain. Most studies have thus focused on the cytological events that accompany development of the grain outer coverings (*19*, *20*). Therefore, the purpose of this study was to provide some chemical insights of the peripheral layers during grain development. To reach this goal, the peripheral tissues of developing wheat grains were obtained at defined ripening stages of the grain and submitted to xylanase hydrolysis. Light microscopy and immunolocalization of the enzyme were used to microscopically explore the maturing peripheral layers and the impact of xylanase. In addition, chemical characterization was undertaken to investigate the structural components of peripheral tissues of the wheat grain, in particular arabinoxylans and the wall phenolics that would potentially limit substrate accessibility (cross-linked hydroxycinnamates and lignin). The protein and lipid fractions were also monitored in relation to the developmental stages.

MATERIALS AND METHODS

Development of Peripheral Tissues of the Wheat Grain. The soft wheat (*Triticum aestivum* cv. Cadenza) was grown in 2002 at Prunay (Reims, northeastern France, 49° 14′ N, 4° 10′ E). Plants for which anthesis (*21*) occurred simultaneously were ringed; this stage corresponds to the onset of grain development. Temperature was measured every hour from anthesis until complete maturity of the grains. Daily mean values were expressed in degrees Celsius per 24 h (°C/day), where only positive temperatures were considered. To evaluate the process of grain maturation, the median part of five spikes was collected daily from the principal stem. The corresponding grains were carefully released from spikelets; glumes and paleae were removed using tweezers. The fresh-matter weight of one grain was estimated as the weight mean value of 60 grains; subsequent dehydration of the grains (48 h at 80 °C) allowed dry matter to be determined. The water contents were calculated from the difference between fresh and dry matter. The main stages of grain development were evidenced from the change in these characteristics on a growing-temperature sum basis.

Isolation of Peripheral Layers from the Wheat Grain. Median parts of the spikes were hand-collected between 8 a.m. and 9 a.m. at specific postanthesis stages, namely, A (183 °C/day), B (384 °C/day), C (672 °C/day), and D (884 °C/day). Spikes were placed in liquid nitrogen, and then samples were stored at −20 °C. Spikes were allowed to thaw overnight at 4 °C before removal of the grains as described above. The grain-ends (brush plus embryo) were discarded with a razor blade; the median part was soaked in distilled water at 4 °C during 2 h for stages B−D to soften the endosperm. This softening step was not required for grains at stage A. An incision in the crease followed by an additional hour of soaking in cold distilled water permitted the removal of the endosperm by scraping the bran under a stereomicroscope. The purity of the endosperm-depleted bran was checked microscopically prior to resin embedding or freeze-drying for biochemical analysis.

Endo-xylanase Preparation. A purified (1→4)-β-endo-xylanase (EC 3.2.1.8) of the glycosylhydrolase family 11 from *Thermobacillus xylanilyticus* culture was used as previously described (*22*). The activity of the (1→4)-β-endo-xylanase was determined following incubation with birchwood xylan (0.5% w/v) for 10 min in 50 mM sodium acetate, pH 5.8, at 60 °C and determination of the reducing sugar using a ferricyanide-based method (*23*). The specific activity of the enzyme was 2000 units/mg of protein. One unit is the amount of xylanase required to release 1 μmol·min^{-1} of reducing equivalent as xylose from birchwood xylan at 60 °C.

Xylanase and Water Treatment of Peripheral Tissues of the Wheat Grain. Xylanase hydrolysis of the peripheral layers isolated at stages A−D was performed in duplicate. Dry samples were hydrated into distillated water (3%, w/v) for 16 h at 60 °C, 10 units/mL of (1→4)-β-endo-xylanase was then added, and the reaction proceeded at 60 °C with constant stirring. After 1 and 2 h (one experiment) and 24 h of incubation, the soluble fractions were retained for analysis and heated at 100 °C (10 min) to stop the reaction. After 10 min of centrifugation at 13000 rpm, supernatants were submitted to acid hydrolysis before sugar analysis. The residual bran was washed twice with water and freeze-dried. Control water incubations of external layers were also performed without xylanase using a similar procedure.

To microscopically examine the effect of the xylanase treatment, grain external layers were incubated (3%, w/v) with a lower amount of enzyme, 0.5 unit/mL, under gentle agitation (Polymax 1040, Heidolph). These conditions allowed the examination of the cytochemical features of the initial steps of the bran degradation, although an optimal yield of arabinoxylan solubilization could have been reached for longer periods, that is, 24 h (*24*). Samples were taken before enzyme addition ($t = 0$) and after 75 min or 24 h of incubation.

Embedding of the Peripheral Tissues of the Wheat Grain. Samples were cut into small pieces under a solution of 2% glutaraldehyde in phosphate buffer (0.1 M, pH 7.4) and fixed in the same reagent for 1 h at room temperature under vacuum. After several washes in phosphate buffer and in distilled water (15 min each), samples were dehydrated in an ethanol series over 48 h, then infiltrated (72 h), and embedded in LR White resin (Sigma) at 60 °C for 24 h. Specimens were cut into semithin sections (0.5 μm thick) using a diamond knife and an HM 360 (Microm) microtome and deposited on glass multiwell slides.

Immunolabeling of the Xylanase. The polyclonal antixylanase antiserum was made by New Zealand white rabbits and produced by Eurogentec. A usual procedure and appropriate buffer were used for xylanase immunolabeling on semithin sections (*2*). Silver enhancement reagents (Amersham Life Science) were applied at room temperature for 7 min. Sections were covered with Eukitt mounting medium (Electron Microscopy Sciences). Immunolabeling controls were carried out in the absence of the primary antibody or the secondary antibody; another control was obtained using water-treated samples to check that labeling specifically corresponded to the tested enzyme. The absence of unspecific binding of silver particles was also checked using unlabeled specimens.

Cytochemistry and Microscopic Observations. Cytochemical staining of semithin sections was achieved using toluidine blue (1% w/v) for 5 min. All observations were performed using an Axioskop microscope (Zeiss) plus an AxioCam MRc digital camera, either with bright light (immunogold and toluidine blue staining) or mercury lamp (UV excitation for phenolic autofluorescence, $\lambda_{excitation} = 340$ nm, $\lambda_{emission} = 430$ nm).

Carbohydrate Analysis. Acid hydrolysis of peripheral tissues (stages A−D) was performed on 5 mg samples previously ground with a ball crusher (Retsh, MM 2000) using 12 M H_2SO_4 (2 h at room temperature) and then 1.5 M H_2SO_4 for 2 h at 100 °C. Analysis of solid samples was performed in triplicate; experimental error was 5%. Soluble fractions recovered from water or xylanase treatment (500 μL) were hydrolyzed for 2 h at 100 °C in the presence of 1 M H_2SO_4. Acid-soluble samples were filtered and injected into a CarboPac PA1 anion exchange column (4 × 250 mm, Dionex). Detection was performed by pulsed amperometry (PAD 2, Dionex). A postcolumn addition of 300 mM NaOH was used. Monosaccharide composition was determined using fucose as the internal standard. Calibration was performed with standard solutions of neutral carbohydrate (arabinose, glucose, xylose, and galactose) and acidic carbohydrate (galacturonic and glucuronic).

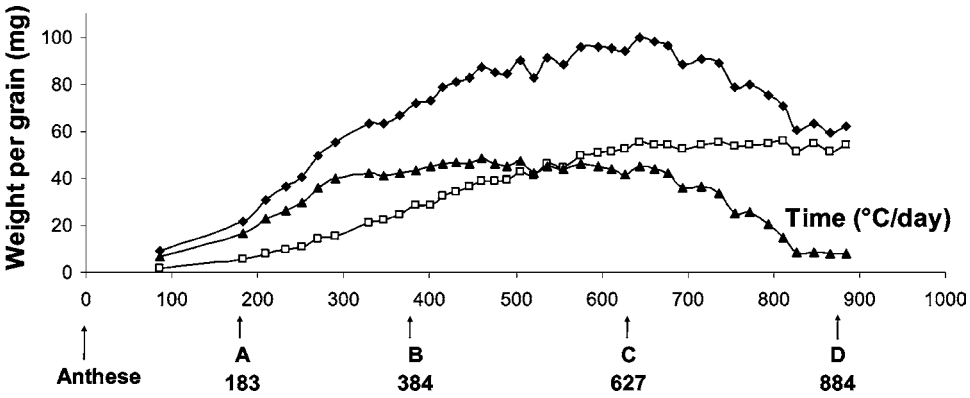

Figure 1. Chronological events of the cv. Cadenza grain development: change in the fresh weight (◆), dry weight (□), and water contents (▲) of individual grains as a function of cumulative growing degrees since anthesis. Relevant harvesting stages are labeled A–D.

The content of arabinoxylan was the sum of the amounts of xylose and arabinose.

Protein Contents. Proteins contents were determined in duplicate by the total N contents (N × 5.7 as an average value of the correcting factor) of 3 mg of ball-milled samples using an elemental analyzer (NA 1500, Carlo Erba) coupled to a mass spectrometer (Fisons Isochrom). The experimental error was <5%.

Phenol Composition of the Peripheral Tissues of the Wheat Grain. Samples were extracted three times at room temperature with 80% ethanol. The residual peripheral tissues of wheat grain were recovered by filtration and then freeze-dried. Olivetol (Aldrich) was added to the combined ethanol fractions prior to evaporation under reduced pressure. The dried extract was dissolved in 2 mL of acetone/methanol (1.4/0.6) and filtered (0.45 μm) prior to injection on a Kromasil 5 μm (RP-18, 250 mm × 4.6 mm) AIT Chromato column. Alkylresorcinols were eluted using a methanol gradient and identified using a photodiode array detector by comparison of reference spectra and elution time (*25*) and were quantified at 280 nm. Data were mean values obtained from duplicate experiments and expressed as equivalents of olivetol with 5% experimental error under the conditions used.

Ester-linked hydroxycinnamates were analyzed after 2 M NaOH treatment (10 mL) of 20 mg of extractive-free peripheral tissues of wheat grain, for 2 h at 35 °C with constant stirring under nitrogen flow. Alkali residues were recovered by centrifugation (13000 rpm, 10 min) and further treated by 4 M NaOH (10 mL) at 170 °C for 2 h to extract ether-linked phenolic acids. Each alkali filtrate was acidified to pH 1, mixed with 3,4,5-trimethoxy-*trans*-cinnamic acid as an internal standard, and extracted three times with 30 mL of ether. The organic phase was dried under reduced pressure and analyzed by HPLC with an elution gradient using a combination of acetonitrile, methanol, and 15 mM orthophosphoric acid in distilled water as previously described (*8*, *24*). Ester- and ether-linked phenolic acids were quantified at 302 nm using commercial standards. Identification and quantification of esterified dehydrodimers were carried out according to UV spectra and retention time with respect to the spectra of 8-*O*-4′-, 5-5′-, and 8-5′-benzofuran dimers. The 8-5′-benzofuran was a gift from X. Rouau (INRA, Montpellier, France); 8-*O*-4′ and 5-5′ forms were formerly purified from an alkali filtrate of wheat bran using preparative HPLC (Novaprep, Merck) and a Lichrospher (Merck, RP-18, 250 mm × 25 mm) column. Determination of ester-linked phenolic compounds was performed in triplicate; variation in the experimental error of monomer and dimer reached 10% owing to the low amount of sample available.

Lignin detection was performed using thioacidolysis that specifically disrupts the noncondensed intermonomer linkages.The reaction was performed in triplicate on 10 mg of extractive-free peripheral tissues of wheat grain samples at 100 °C using ethanethiol/BF_3etherate/dioxane reagent as detailed previously (*26*). After a 4 h reaction, the mixture was diluted with water containing tetracosane as an internal standard and extracted with dichloromethane. Guaiacyl (G) and syringyl (S) thioethylated monomers were analyzed as their trimethylsilyl derivatives using a gas chromatograph equipped with a fused silica capillary DB1 column (30 m × 0.3 mm) and a flame ionization detector. The temperature gradient was 160−200 °C at 3 °C/min (*26*). Due to the low amount of lignin analyzed, the experimental error (≤10%) was higher than usually obtained on highly lignified samples (*26*).

Lipid Analysis. Aliphatic compounds were released as methyl esters of fatty acids by transesterification using 10% BF_3 in dry methanol (*27*). The reaction was performed in triplicate, and samples (3 mg) were left to react in 3 mL of reagent for 24 h at 70 °C. The methanol extract was removed and the residue washed three times in chloroform. The combined organic phase was washed in a NaCl-saturated solution and dried over Na_2SO_4. Monomers were converted to their trimethylsilyl ethers prior to analysis by gas chromatography as above using a temperature gradient kept at 120 °C for 8 min and then elevated to 300 °C at 2 °C/min. Aliphatic monomers were identified using GC-MS with respect to reference spectra reported elsewhere and to fragmentation pattern (*27*−*29*). The analytical measurement of aliphatic compounds was 5%.

RESULTS AND DISCUSSION

Microscopic View of Peripheral Tissues of Maturing Wheat Grain. Fresh and dry matters of the grain were determined daily over a period of ∼50 days. These values are plotted in **Figure 1** on a growing-temperature sum basis. The experimental data allowed the selection of pertinent stages of grain development with respect to the physiological and cytological events of grain maturation (*4*, *30*).

The micrographs of stage A are shown in **Figure 2a**,**b**. At this stage (183 °C/day or 11 day postanthesis) the grains were very small and green; the external layers were clearly distinguished. All of the cells had a large cytoplasm, which considerably contrasts with the crushed aspect of mature peripheral tissues of wheat grain. Cell walls occurred as thin and floppy layers, especially at the aleurone layer. This stage corresponds to an active proliferation of endosperm cell and to aleurone differentiation (*4*, *31*). The testa (in **a**) and the pericarp (in **b**) were distinguishable, which agrees with previous studies (*18*, *32*). At stage B (384 °C/day, 20 days after anthesis), water uptake has stopped (**Figure 1**), indicating reserve accumulation in the green grains. All peripheral tissues of the wheat grain could be observed. The testa cellular layer was not yet crushed (**Figure 2c**) because the partially filled endosperm cannot exert a strong pressure on the external layers. The nucellar layer (nl) was fully expanded as some space between the two walls was easily seen (**Figure 2d**). At this stage, the cuticles of both the testa and nucellar layer as well as cross cells and tube cells (the last ones being not visible on the microphotographs) were fully differentiated as previously reported (*33*). The cytoplasm of cross cells began to degenerate in the vicinity of some persisting thin-walled cells (arrow in **Figure 2c**). Stage C (627 °C/day, 37 days after anthesis) corresponds to the cessation of starch and water accumulation in the endosperm. Grains turned

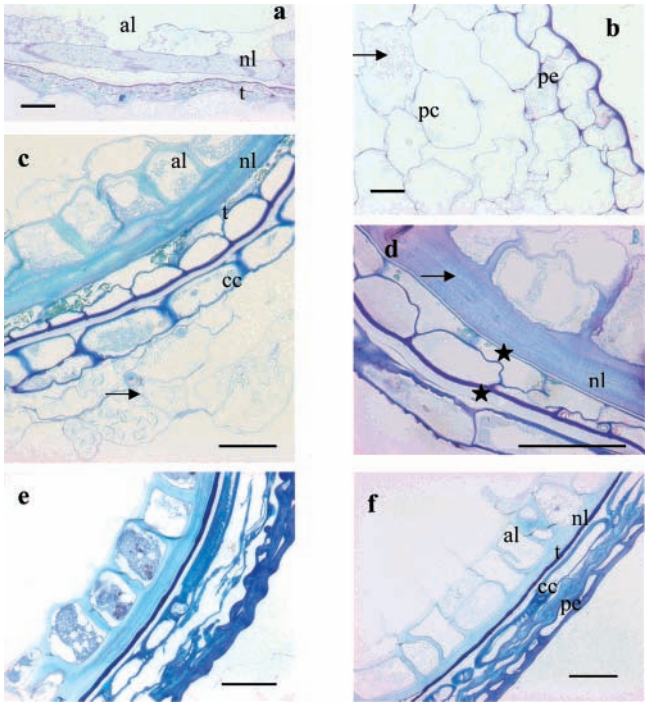

Figure 2. Micrographs of the peripheral tissues of wheat grain sections isolated at different development stages stained by toluidine blue. This topochemical reagent enlightens the histological features of peripheral tissues of wheat grain from stage A, where the aleurone and nucellar layers can be observed as well as cells that prefigure the future testa (**a**) and the pericarp is not yet crushed (**b**). The arrow in **b** spots the presumably starch granules accumulation in the pericarp parenchymatous cells. Toluidine blue staining of stage B (**c** and **d** at, respectively, $t = 0$ and 24 h of water treatment) shows the complete (the tube cells are not visible) but immature structure of peripheral tissues of wheat grain. In **c** the arrow indicates some vestige of persisting thin cell wall. Additionally, these two pictures can be considered as a control, because no structural change was observable during the 24 h water incubation. In **d** the arrow indicates the space inside the nucellar walls, and the stars indicate the cuticles of both testa and nucellar layer. In **e** (stage C at $t = 0$ h) and **f** (stage D at $t = 0$ h) the mature aspect of peripheral wheat layers was distinguishable. al, aleurone layer; nl, nucellar layer; t, testa; cc, cross cells; pc, parenchymatous cells; pe, external pericarp. Scale bars = 40 μm.

brown and reached their maximal weight; external layers appeared to be quite similar to peripheral tissues of mature wheat grain (**Figure 2e**). The nucellar layer was now crushed, and cross cells had lost their photosynthetic activity as previously described (*19*), the only living cells were the aleuronic ones. At stage D (884 °C/day, 49 days after anthesis) the water contents had substantially decreased; the grains were completely brown and the volume had declined. The grain was considered to be mature, and the section shown in **Figure 2f** was equivalent to earlier published microphotographs of mature wheat bran (two among numerous ones, refs *2* and *30*).

Chemical Aspect of Peripheral Tissues of Maturing Wheat Grain. The chemical composition of the peripheral layers of the maturing grain was assessed on three distinct samples. A significant reduction in the protein contents was noticed between stages A and B (**Table 1**) and could result from a much weaker metabolic activity at stage B. Thereafter, the protein levels slightly increased until stage D; these proteins are presumably part of the aleurone cells (*4*). The levels of aliphatic components in the extracted peripheral tissues of wheat grain showed a marked rise between stage A and later stages. This trend could correspond to the differentiation of the polyester-rich cuticular layers at stage B as observed microscopically. From stage B to grain ripeness, the percentage of aliphatics slightly decreased (**Table 1**). Moreover, alkane monomer composition that was attained by depolymerization through transesterification displayed dramatic changes between stages A and B. Hydroxylated derivatives were prevalent in the external layers at stage A, whereas, at later stages, fatty acids accounted for nearly 80% of the transesterification products. The C16 and C18 fatty acids and hydroxylated derivatives were the main monomers as previously reported in mature wheat bran (*5*). The 9,10-epoxy-C18 hydroxyoctadecanoic acid, usually encountered in cutin, was found in rather low proportions (7% of total aliphatic). However, epoxy derivatives might be unstable during transesterification and could be underestimated in our study (*28*). The dicarboxylic derivatives and long-chain hydroxylated acids (>C20), which are reported as diagnostic features of suberin (*29*), were found at only trace level, in agreement with the aliphatic composition of wheat bran. Cereal alkylresorcinols are phenolic lipids containing 17−25 carbons in the aliphatic chains. The C19 and C21 alkyresorcinols were the major homologues in the peripheral tissues of maturing wheat grain (**Table 1**) as for mature grain (*34*). The contents of alkylresorcinol strongly increased from 20-day-aged grains. The proportions then significantly declined during maturation in accordance with a previous report on the whole cereal grains (*25*). The aliphatic fraction and alkylresorcinols of peripheral tissues of wheat grain thus displayed similar profiles across ripening of the grain. These quantitative variations might indicate that the outer layers should undergo some rearrangements until the grain matured.

Carbohydrate analysis of the peripheral tissues of wheat grain led to similar amounts of total neutral sugar irrespective of their maturation stage (**Table 2**). However, the arabinoxylan content at stage A was ~3-fold less than those measured at later stages. Indeed, glucose accounted for nearly 74% of the neutral sugar at stage A, consistent with the observation of many granules in the pericarp parenchymatous cells (**Figure 2b**). The carbohydrate contents determined at stage A should mostly reflect intracellular compounds such as starch granules. In contrast,

Table 1. Protein, Aliphatic Components, and Alkylresorcinol Contents of Peripheral Tissues of Developing Wheat Grain

	maturation stage			
	A	B	C	D
protein[a]	12.0	9.2	10.0	11.3
aliphatic components[a]				
MePalmitate, C16	nq[b]	0.26	0.31	0.23
MeStearate, C18	nq	0.28	0.22	0.21
MeOleate, C18:1	0.19	2.90	1.75	1.43
MeLinoleate, C18:2	0.33	6.56	5.94	5.31
C16 (OH)	0.51	0.48	0.33	0.39
C18:1 (OH)	0.69	0.97	0.92	0.68
C16 di-OH	nq	nq	0.12	0.12
C18 tri-OH	nq	nq	0.10	0.10
C18 di-OH 9-epoxy	0.42	0.85	0.81	0.66
alkylresorcinols[c]				
C17	59	216	64	62
C19	nq	807	328	343
C21	21	966	348	467
C23	236	348	56	107
C25	nq	72	nq	42

[a] Expressed as weigh percentage of dry matter. [b] Not quantifiable. [c] Expressed as μmol of equivalent olivetol/g of extractive-free peripheral tissues of wheat grain. Standard deviation averaged 5% for protein, aliphatic components, and alkylresorcinols.

Table 2. Carbohydrate Composition of Peripheral Tissues of Developing Wheat Grain[a]

maturation stage	neutral carbohydrate								
	Ara	Gal	Glc	Xyl	TNCC	A/X	AX[b]	Glc Ac	Gal Ac
A	6.01	1.59	41.7	7.32	56.7	0.82	23.6	0.23	0.45
B	13.8	1.17	18.6	23.3	56.8	0.58	65.1	1.04	0.80
C	14.2	1.11	19.5	23.7	58.5	0.59	64.8	1.08	0.79
D	13.2	1.19	18.0	21.5	53.9	0.61	64.4	1.01	0.69

[a] Contents are expressed in weight percentage of dry matter, except for AX. Abbreviations: Ara, arabinose; Gal, galactose; Gal Ac, galacturonic acid; Glc, glucose; Glc Ac, glucuronic acid; Xyl, xylose; AX, % Ara + % Xyl; A/X, arabinose-to-xylose ratio; TNCC, total neutral carbohydrate contents. [b] Expressed as a percentage of the total neutral carbohydrate contents (Ara + Gal + Glc + Xyl). Standard deviation averaged 5%.

Table 3. Cell-Wall Phenolic Components of Peripheral Tissues of Developing Wheat Grain[a]

		maturation stage			
		A	B	C	D
hydroxycinnamic acids[b]					
ester	FA	4750	12590	9607	4519
	pCA	nq	205	249	180
ether	FA	128	113	401	333
	pCA	135	106	244	201
	SA	106	80	132	93
ester-DHD	5,5′	nq	58	62	71
	8-*O*-4′	nq	165	168	174
	8,5′	nq	57	60	53
lignin[c]					
	total S + G	nd	nd	4.8	4.3
	S/G molar ratio	nd	nd	0.8	0.8

[a] Abbreviations: FA, ferulic acid; pCA, *p*-coumaric acid; SA, sinapic acid; DHD, dehydrodimer; nd, not detectable; nq, not quantifiable. [b] Expressed as μg/g of extractive-free peripheral tissues of wheat grain. [c] Total yields of labile-ether linked guaiacyl (G) and syringyl (S) derivatives expressed as μmol/g of extractive-free peripheral tissues of wheat grain. Standard deviation averaged 15% for lignin monomer and 10% for hydroxycinnamate.

the glucose proportion strongly decreased at stages B−D and may have originated from cellulose and β-(1−4,1−3) glucans; AX represented ~65% of the neutral sugar. The A/X ratio was close to 0.60, indicating a high substitution degree. This feature remained constant from stage B, as did the contents and composition of neutral sugars. Uronic acids are minor components of graminaceous cell walls and accounted for only 1.5% of the wheat bran at physiological maturity stage. A slight reduction in the galacturonic acid contents (14%) was observed over the grain maturation (**Table 2**). Apart from stage A, the carbohydrate contents and the composition of the grain peripheral tissues were quite similar during grain maturation and provided values consistent with literature data on industrial bran (*4*, *18*).

Wall-bound phenolic acids were predominant in the grain external layers because the ethanol-soluble hydroxycinnamates represented <0.08% of the peripheral tissues of wheat grain (data not shown). Following successive alkaline hydrolyses of the extractive-free peripheral tissues of wheat grain, we estimated the contents in ester- and ether-linked phenolic acids (**Table 3**). The data presented herein only concern the trans form; trace levels of cis isomers were found as previously described (*35*, *36*). FA was the major phenolic monomer in the peripheral tissues of wheat grain at all development stages; pCA and SA occurred in much lower proportions. Particularly, SA was quantified only as its ether derivative. Except for the esterified FA, hydroxycinnamate monomer profiles exhibited similarities throughout wheat grain development. Indeed, their contents were in the same range and got increasing values from stage B to stage C, when grains reached their maximal weight. At mature stage (D), slightly lower proportions were recovered after alkaline hydrolysis. These data were consistent with previous studies on phenolic changes in the whole maturing grain of *T. aestivum* (*35*−*38*). On the contrary, esterified FA was largely predominant and reached highest levels at stage B, at which time the proportion of esterified FA then decreased until the maturity stage (D). Several hypotheses have been suggested to explain the great variation in FA concentrations. The rise in ferulic acid synthesis has been associated with significant levels of phenylalanine ammonia-lyase at the early stage of grain formation, after which peroxidase that occurs in the outer coverings would induce the formation of covalent cross-links between wall polymers (*36*, *37*). Therefore, ferulate could be involved in other structures such as diferulic dehydrodimers (*36*). We thus checked whether changes in FA levels were connected to DHD and lignin accumulation (*39*, *40*). Many kinds of DHD occur in graminaceous cell walls, 5,5′, 8-*O*-4′ and 8,5′ derivatives being the most frequent ones in industrial bran (*41*). At stage A, DHD were found at trace levels (**Table 3**), but noticeable amounts were quantified at the latest stages, in agreement with literature data. However, the DHD contents were identical from the onset of the hydrical step up to the latest stage. Compensation for the loss of esterified FA would thus hardly rely on the formation in the three dehydrodimers presented here. Nevertheless, it should be pointed out that owing to the prevalent contribution of ferulate in cross-linking lignin and polysaccharide in graminaceous (*12*), part of the ferulate monomer and DHD cannot be measured by current solvolytic methods. Indeed, several studies have reported that ferulates and diferulates act in graminaceous cell walls as nucleation or initiation sites for lignification. As an example, DHD accumulation in wheat bran did not compensate for the decrease in FA contents following UV irradiation, suggesting formation of new cross-linkage between lignin and hemicellulose (*42*). Due to limited quantities of microdissected peripheral tissues of wheat grain samples, lignin contents were not determined by typical procedures. However, lignin could be monitored in the peripheral tissue samples of maturing grains at stages C and D using thioacidolysis that liberates syringyl and guaiacyl lignin monomers involved in β-*O*-4 labile-ether linkages (**Table 3**). Earlier cytochemical studies have already suggested late lignin deposition in the pericarp during grain maturation, although chemical diagnostic features were not provided. Thioacidolysis cleaves the labile aryl−alkyl-ether linkages, thereby allowing the characterization of the so-called uncondensed lignin fraction (*43*). Total yields (S + G) were very low due to the weak proportion of lignin as previously reported (*44*) and did not show a significant variation between the developmental stages C and D. The proportion of labile-ether-linked lignin structures within the total lignin can be estimated by assuming that thioacidolysis disrupts nearly 100% of the β-*O*-4 bonds, that the average molar mass of the lignin monomers is 200, and that a 4% maximum lignin content can be estimated from the data obtained in our laboratory on industrial bran (*24*). The uncondensed lignin fraction would thus represent <10% of the polymer, suggesting the deposition of a highly condensed lignin in peripheral tissues of wheat grain. The weak S/G ratio further argued for a condensed lignin type, which is often described as guaiacyl-enriched polymer (*45*). Altogether, the data on the bound

phenolic fraction suggest that progressive bonding patterns should operate in the cell walls during grain maturation.

Microscopic View of Peripheral Tissues of Wheat Grain Degradation. A pure thermostable xylanase was used to explore potential changes in the cell wall network of the external layers isolated from developing grain. For this, microscopic and chemical data of xylanase-depleted peripheral tissues of wheat grain were compared to those of untreated and water-treated samples.

Peripheral tissues of wheat grain samples were microscopically assessed following short (75 min) and longer incubation times (24 h); however, the most relevant changes that had already occurred after a 75 min enzyme treatment were illustrated. In addition, owing to the marked brittleness of the enzyme-treated samples at stage A, this study mainly informed on histological events occurring in samples collected at stages B−D. Cytochemical alterations were investigated using toluidine blue staining and UV-autofluorescence of hydroxycinnamates (*46*). In addition, xylanase immunolabeling enabled localization of the enzyme within the peripheral layers of wheat grain during hydrolysis. Immunocytochemical controls did not give detectable labeling of xylanase, indicating a specific xylanase labeling of cell walls. Indeed, the antixylanase serum did not react with control peripheral layers as shown, for instance, for the samples collected at stages B and D (**Figure 3g**,**h**). Moreover, no xylanase labeling was detected using secondary antibodies alone or silver enhancement (picture not shown).

Toluidine blue staining of peripheral tissues of wheat grain at stage B showed collapsed aleurone and altered nl after 75 min of xylanase treatment (**Figure 3a**). The nucellar layer, which was partially detached, and the aleurone cell walls were heavily labeled with gold particles after silver enhancement (**Figure 3b**). Therefore, xylanase had penetrated in these cellular layers, inducing significant histological changes. In contrast, the other tissue layers did not react with xylanase antibodies and kept their cell integrity. Likewise, similar changes were obtained after 75 min of xylanase treatment of peripheral tissues of wheat grain at stage C, when only the aleurone cell walls and nucellar layer were labeled. However, xylanase immunolabeling occurred in a more restricted area within the nl (**Figure 3d**). At stage D, cytochemical alterations of the al layer and nl were similar as shown in **Figure 3e**; the gap between external and inner pericarp observed in this photograph was not linked to the xylanase treatment. The immunolabeling of xylanase was encountered again only on the aleurone cell walls and nl (**Figure 3f**).

The cell walls of the remaining al displayed a weak blue autofluorescence in small domains when the specimen from the sample at stage C was exposed to UV light (**Figure 3c**). For comparison, a strong blue fluorescence was observed in the 24 h water treatment sample (**Figure 4c**), indicating the widespread distribution of ferulate in peripheral tissues of wheat grain controls. Likewise, the blue fluorescence was present mainly in the al cell walls and remained so throughout grain maturation (**Figure 4a**,**b**, stage B; **Figure c**,**d**, stages C and D). Similar patterns of autofluorescence were observed in the untreated peripheral tissues of wheat grain, indicating that water treatment did not induce any marked microscopic change for all of the maturation stages (data not shown). In contrast, all samples had a weakened aleurone fluorescence following xylanase treatment. Consistently, previous studies reported on the loss of UV blue autofluorescence from aleurone walls when degraded by hydrolytic enzyme (*18*, *47*). The in situ xylanase location was even shown to be closely connected to AX degradation and the disappearance of bran autofluorescence (*2*).

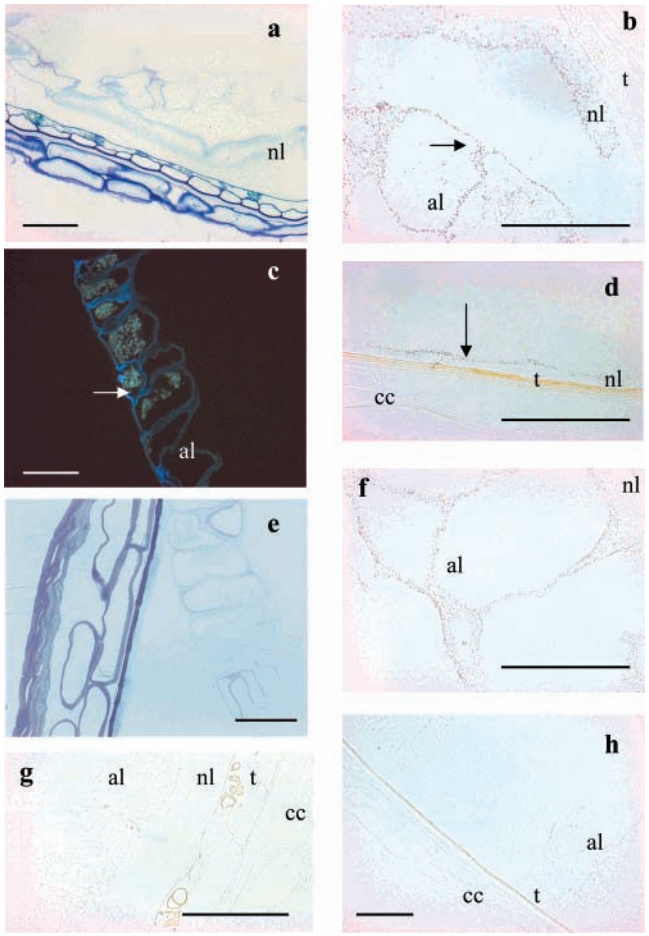

Figure 3. Micrographs of sections of 75 min xylanase-depleted peripheral tissues of wheat grain isolated at different development stages and xylanase immunolabeling controls. Pictures **a** and **b** are, respectively, toluidine blue staining and xylanase immunolabeling of peripheral tissues of wheat grain at stage B. The arrow in **b** indicates the heavy xylanase immunolabeling as visualized by gold particles. In **d** the xylanase immunolabeling of peripheral layers of wheat grain at stage C (black arrow) shows a wave of gold particles in the nl. In addition, for stage C, the picture **c** displays phenolic UV-autofluorescence in restricted cell-wall domains under UV light (white arrow). Pictures **e** and **f** are stage D, respectively, stained by toluidine blue and labeled by xylanase antibodies. Xylanase-immunolabeling controls show the absence of gold particles (**g**) when peripheral tissues of wheat grain (stage B) are not incubated with xylanase and (**h**) following omission of the primary antibody (stage D). al, aleurone layer; nl, nucellar layer; t, testa; cc, cross cells. Scale bars = 40 μm.

A 24 h enzyme incubation did not induce visible change of the peripheral tissues of wheat grain other than aleurone cell walls or nl (data not shown); these layers were finally detached from the testa. No labeling of xylanase could be observed in the residual tissues. Overall, histological features did not outline a clear-cut effect of the grain development from 384 to 884 °C/day on the way xylanase degrades peripheral tissues of wheat grain. Aleurone and nucellar layers were target cells, and pericarp and testa remained recalcitrant as shown for industrial bran (*18*). Nevertheless, xylanase immunolabeling allowed pinpointing in the formation of nucellar lysate from stage B to later ones. Indeed, xylanase immunolabeling highlighted a dense layer at stage C that was not found on B (compare **b** and **d** in **Figure 3**). This thin amorphous layer interfaces with aleurone and nl and likely originates from the nucellus crushing (*1*).

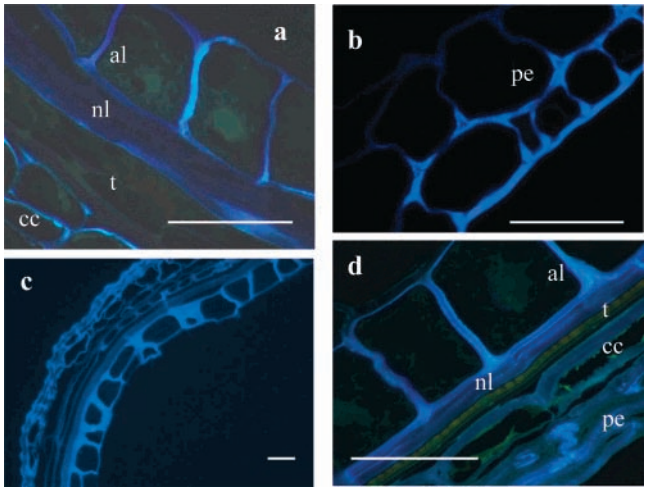

Figure 4. Micrographs of peripheral tissues of wheat grain sections isolated at different development stages under UV lamp; examination of the wall phenol-linked autofluorescence with UV light exposure of peripheral layers of wheat grain obtained at stages B (**a** and **b**), C (**c**), and D (**d**). All of the pictures present a blue fluorescence of tissues after 24 h of water treatment, especially in the aleurone cell walls. al, aleurone layer; nl, nucellar layer; t, testa; cc, cross cells; pe, external pericarp. Scale bars = 40 μm.

Table 4. Yields of the Neutral Carbohydrate Components Released from Peripheral Tissues of Developing Wheat Grain Following Water and Xylanase Treatments[a]

maturation stage	water incubation		xylanase incubation		
	0 h[b]	24 h[c]	1 h[d]	2 h[d]	24 h[c]
A	35.2 ± 3.60	35.7 ± 5.31	nm	nm	40.8 ± 2.69
B	1.71 ± 0.31	2.25 ± 0.10	19.8	22.2	22.9 ± 0.40
C	1.84 ± 0.29	1.96 ± 0.16	17.1	17.3	22.2 ± 0.96
D	2.11 ± 0.17	2.16 ± 0.08	16.2	18.7	20.5 ± 1.72

[a] Contents were expressed as a weight percentage of the initial peripheral tissues of wheat grain dry matter. Abbreviation: nm = not measured. Data are mean values ± SD. [b] $n = 4$. [c] $n = 2$. [d] Only one experiment.

Interestingly, xylanase was previously shown to behave distinctively in the nucellar lysate of industrial bran (*2*).

Chemical Aspect of Xylanase Efficiency. Chemical analysis was performed on the most relevant components regarding enzyme efficiency. At first, the yields of soluble carbohydrates, especially AX products, were determined following water and xylanase treatments (**Tables 4** and **5**). The proportion of water-soluble carbohydrate was very high at stage A and should mainly corresponds to the release of glucose-rich components from intracellular components (see above). Also, a large variation in experimental results was obtained and likely arose from the heterogeneous and partial deposition of aleurone at stage A. Conversely, water control released small amounts of carbohydrates from the peripheral tissues of wheat grain isolated at later stages (~2% of the initial dry matter) without any noticeable changes over 24 h (**Table 4**). The content of water-soluble carbohydrate was consistent with previous data on industrial bran, although the proportion of AX appeared low in stage D (**Table 5**).

When compared to the water incubation, a 24 h xylanase treatment from stage A allowed the recovery of a slightly higher amount of soluble compounds. Longer incubation did not lead to higher degradation (data not shown). In contrast, following addition of xylanase to samples collected at stages B−D, the proportion of soluble carbohydrates increased significantly and

Table 5. AX Content and A/X Ratio of the Soluble Products Released from Peripheral Tissues of Developing Wheat Grain Following Water and Xylanase Treatments[a]

maturation stage		water incubation		xylanase incubation		
		0 h[b]	24 h[c]	1 h[d]	2 h[d]	24 h[c]
A	AX (%)	3.93 ± 1.78	5.03 ± 1.01	nm	nm	12.0 ± 1.13
	A/X	0.46 ± 0.03	0.42 ± 0.07			0.44 ± 0.06
B	AX (%)	29.2 ± 6.12	30.0 ± 4.77	83.7	81.8	77.9 ± 2.69
	A/X	0.71 ± 0.08	0.67 ± 0.06	0.24	0.24	0.23 ± 0.01
C	AX (%)	49.5 ± 2.26	52.6 ± 2.90	88.8	88.4	85.6 ± 1.60
	A/X	0.54 ± 0.03	0.52 ± 0.02	0.28	0.27	0.27 ± 0.03
D	AX (%)	12.1 ± 1.07	12.3 ± 0.31	81.5	81.4	77.9 ± 4.26
	A/X	0.57 ± 0.03	0.59 ±0.03	0.30	0.28	0.27 ± 0.03

[a] Results were expressed as a percentage of the total soluble-neutral carbohydrate. Abbreviations: AX, % Ara + % Xyl; A/X, arabinose-to-xylose ratio; nm, not measured. Data are mean values ± SD. [b] $n = 4$. [c] $n = 2$. [d] Only one experiment.

reached maximum levels after 2 h of xylanase incubation, indicating a rather fast enzymatic hydrolysis of the peripheral tissues of the wheat grain. No evidence of variation in the time course of the carbohydrate release was seen between samples (**Table 4**). Therefore, xylanase incubation was responsible for the release of nearly 20% of the carbohydrate of the initial dry matter. In contrast to stage A, for which AX accounted for only 12% of the soluble fraction, AX represented nearly 80% of the carbohydrate released from the other samples (**Table 5**), which confirmed that AX were efficiently disrupted by xylanase. This degradation induced dry matter losses that reached 40, 41, and 43% following enzymatic treatment of the peripheral tissues of wheat grain isolated at stages B, C, and D, respectively. Enzyme-soluble AX were characterized by a low A/X ratio. These values agree well with previous data on the treatment of mature industrial wheat bran using similar enzyme (*2*, *18*). The A/X ratio reflected the substitution degree of the xylooligosaccharide and did not vary significantly during xylanase treatment. On average, grain peripheral tissue-released AX harbored one arabinose for four xylose and did not change depending on the grain maturation stage. This lack of variation suggests that rearrangement of the xylanase target structures during maturation, if any, would not substantially affect enzyme efficiency.

Enzyme-depleted peripheral tissues of wheat grain were further characterized regarding components that cross-link AX and potentially hinder substrate accessibility. In this respect, wall-bound phenolic compounds were mainly investigated. The relative proportions of hydroxycinnamates and of uncondensed monolignols are expressed as a percentage of their initial contents in the untreated samples (**Table 6**). No significant loss in the uncondensed lignin fraction was noticed following xylanase action; accordingly, the molar ratio S/G stayed unchanged in the residual peripheral tissues of wheat grain (stage C or D). This trend is consistent with the preferential lignin distribution in pericarp (*44*), which did not show visible alteration under xylanase. On the whole, ether-linked hydroxycinnamates were less removed than the ester ones. Furthermore, the contents of residual esterified FA strongly decreased during the development stage, whereas similar proportions of etherified FA were recovered in residual peripheral tissues of wheat grain. When compared to FA, the wall-bound pCA and SA were released in highest proportions irrespective of the kind of peripheral tissues of wheat grain. Variation in the yields of phenolic acid monomers remaining after enzyme degradation indicates that distribution and cross-linkage patterns may change

Table 6. Recovery Yield of Phenolic Components in the Xylanase Residues of Peripheral Tissues of Developing Wheat Grain[a]

		maturation stage			
		A	B	C	D
hydroxycinnamates					
ester	FA	37	65	49	39
	pCA	nd	14	24	25
ether	FA	11	84	75	91
	pCA	19	57	45	49
	SA	12	53	55	64
ester DHD	5,5′	nq	83	101	93
	8-*O*-4′	nq	116	11	120
	8,5′	nq	94	108	83
lignin					
	total S + G	nd	nd	95	114
	S/G molar ratio	nd	nd	0.8	0.9

[a] Abbreviations: FA, ferulic acid; pCA, *p*-coumaric acid; SA, sinapic acid; DHD, dehydrodimer; G, guaiacyl; S, syringyl; nq, not quantifiable; nm, not measured. Recovery yield expressed in percentage of initial contents in untreated peripheral tissues of wheat grain.

according to peripheral layers and/or maturation stage. As a matter of fact, esterified FA decreased from stage B to stage D and appeared to be more extractable to enzyme treatment. In contrast to hydroxycinnamate monomers, DHD were concentrated in the xylanase residue from stages B−D and were even quantified in the degraded peripheral layers of wheat grain corresponding to stage A. On the basis of estimation of the dry matter loss induced by enzyme treatment and assuming that no DHD were released from the weak proportion of cell walls, DHD roughly represents 130 μg/cell wall g. This means that bran DHD are deposited at a very early stage of the grain formation. Considering that pericarp undergoes a very weak lignification at more advanced stages, DHD may significantly consolidate immature peripheral tissues of wheat grain cell walls into mature ones prior to lignin deposition as previously suggested in wheat seedling (*48*).

Among peripheral tissues of wheat grain, xylanase led to the depletion of mostly aleurone and nl. The composition of enzymatic hydrolysates thus mostly reflected the degradation of these target structures that are rich in low-substituted AX (*18*). However, subcellular chemical heterogeneity cannot be excluded. Nucellar lysate was thus the latest altered layer. Additionally, the thin inner aleurone cell walls, which are not degraded by xylanase (*2*), contain structural proteins that can cross-link with DHD (*49*). Conversely, the chemical features of enzyme-depleted peripheral tissues of wheat grain largely account for the resistant outermost layers that are rich in lignin, cellulose, DHD, and highly substituted AX. Altogether, chemical and cytochemical data argued for similar xylanase efficiencies in the external layers isolated at various growing stages. Considering the preferential xylanase degradation of aleurone and nl, one can suggest that potentially hampering structures are deposited early in these target layers. Our results also showed that pericarp and testa layers are already enzyme-recalcitrant at stage B when uncondensed lignin was not detected. Therefore, the degree of xylan substitution and the cross-linkage pattern must be the main relevant factors in xylanase efficiency. In this respect, DHD are detected at the early stages of grain maturation and did not further vary. This could explain to some extent that maturing peripheral tissues of wheat grain are similarly degraded. The biodegradability of highly lignified graminaceous cell walls was reported to decline during plant maturity. Several factors are involved, notably hydroxycinnamate interconnecting lignin and hemicelluloses and pCA linkage to lignin, which are key factors that impede wall disassembly. In comparison, neither high deposition of pCA nor intense lignification accompanies maturation of the external layers of the grain, supporting the fact that DHD cross-linking would mainly contribute to the resistance of wheat grain against enzymatic degradation. In this respect, further studies are needed to get a better understanding of the various forms of hydroxycinnamates that occur in peripheral tissues of grain, as recently illustrated by the isolation of a ferulate dehydrotrimer and sinapate dimers (*50*, *51*). In cereal bran, deposition of ferulate dimers could display tissue-specific patterns with respect to the high level of DHD in pericarp. Further studies are on the way to gain a more comprehensive view of the chemical events related to maturation of the peripheral tissues of wheat grain using individual microdissected layers. Moreover, it is noteworthy that results reported in this study concern only peripheral tissues from the central portion of the wheat grain, including a small proportion of crease material for which composition may differ from the rest of the grain surrounding layers. This material was distinguishable from milling bran fractions, which comprise the poles of the grain; therefore, comparison with the whole bran would need some care. In addition, studies on the early stage of grain formation would improve our understanding of the initial steps of the substitution pattern of arabinoxylans that must occur in the outer layers for a few days after anthesis.

Our chemical results provide significant insight regarding the chemical evolution of the peripheral tissues of wheat grain with emphasis on xylanase degradation. Nevertheless, taking into account the significant chemical variability of wheat brans (*8*, *10*), this study, which focused on one wheat cultivar, would require further investigation regarding genetic and environmental effects on the development of the grain outer coverings.

ABBREVIATIONS USED

al, aleurone; AX, arabinoxylans; DHD, dehydrodimers; FA, ferulic acid; G, guaiacyl; nl, nucellar layer; pCA, *p*-coumaric acid; SA, sinapic acid; S, syringyl; xylanase, (1→4)-β-endoxylanase.

ACKNOWLEDGMENT

We thank Marthe Carlier for skillful technical assistance and Dr. X. Rouau for providing 8-5′-benzofuran.

LITERATURE CITED

(1) Evers, A. D.; Reed, M. Some novel observations by scanning electron microscopy on the seed coat and nucellar layer of the mature wheat grain. *Cereal Chem.* **1988**, *65*, 81−85.

(2) Beaugrand, J.; Reis, D.; Guillon, F.; Debeire, P.; Chabbert, B. Xylanase-mediated hydrolysis of wheat bran. Evidence for subcellular heterogeneity of cell walls. *Int. J. Plant Sci*. **2004**, in press.

(3) Shetlar, M. R. Chemical study of the mature wheat kernel by means of the microscope. *Cereal Chem.* **1948**, *25*, 99−110.

(4) Evers, T.; Millar, S. Cereal grain structure and development: some implication for quality. *J. Cereal Sci.* **2002**, *36*, 261−284.

(5) Matzke, K.; Riederer, M. The composition of the cutin of the caryopses and leaves of *Triticum aestivum* L. *Planta* **1990**, *182*, 461−466.

(6) Fincher, G. B.; Stone, B. A. Cell walls and their components in cereal grain technology. In *Advances in Cereal Sciences*; Pomeranz, Y., Ed.; AACC: St. Paul, MN, 1986; Vol. 8, pp 207−295.

(7) Ebringerová, A.; Hromádková, Z. Xylans of industrial and biomedical importance. *Biotechnol. Genet. Eng. Rev.* **1999**, *16*, 325−341.
(8) Beaugrand, J.; Crônier, D.; Debeire, P.; Chabbert, B. Arabinoxylan and hydroxycinnamate content of wheat bran in relation to endoxylanase susceptibility. *J Cereal Sci* **2004**, in press.
(9) Hartley, R. D.; Morrisson, W. H.; Himmelsbach, D. S.; Borneman, W. S. Cross-linking of cell wall phenolic arabinoxylans in graminaceous plants. *Phytochemistry* **1990**, *29*, 3705−3709.
(10) Lempereur, I.; Surget, A.; Rouau, X. Variability in dehydrodiferulic acid composition of durum wheat (*Triticum durum*) and distribution in milling fractions. *J. Cereal Sci.* **1998**, *28*, 251−258.
(11) Chesson, A. Lignin-polysaccharide complexes of the plant cell wall and their effect on microbial degradation in the rumen. *Anim. Feed Sci. Technol.* **1988**, *21*, 219−228.
(12) Hatfield, R. D.; Ralph, J.; Grabber, J. H. Cell wall cross-linking by ferulates in grasses. *J. Sci. Food Agric.* **1999**, *79*, 403−407.
(13) Lam, T. B. T.; Iiyama, K.; Stone, B. A. Hot alkali-labile linkages in the walls of the forage grass *Phalaris aquatica* and *Lolium perenne* and their relation to in vitro wall digestibility. *Phytochemistry* **2003**, *64*, 603−607.
(14) Scalbert, A.; Monties, B.; Lallemand, J.-Y.; Guittet, E.; Rolando, C. Ether linkage between phenolic acids and lignin fractions from wheat straw. *Phytochemistry* **1985**, *24*, 1359−1362.
(15) Lam, T. B.-T.; Iiyama, K.; Stone, B. A. Cinnamic acid bridges between cell wall polymers in wheat and phalaris internodes. *Phytochemistry* **1992**, *31*, 1179−1183.
(16) Rhodes, D. I.; Sadek, M.; Stone B. A. Hydroxycinnamic acids in walls of wheat aleurone cells. *J. Cereal Sci.* **2002**, *36*, 67−81.
(17) Izydorczyk, M. S.; MacGregor, A. W. Evidence of intermolecular interactions of β-glucans and arabinoxylans. *Carbohydr. Polym.* **2000**, *41*, 417−420.
(18) Benamrouche, S.; Crônier, D.; Debeire, P.; Chabbert, B. A chemical and histological study on the effect of (1→4)-β-endoxylanase treatment on wheat bran. *J. Cereal Sci.* **2002**, *36*, 253−260.
(19) Cochrane, M. P.; Duffus, C. M. Morphology and ultrastructure of immature cereal grains in relation to transport. *Ann. Bot.* **1979**, *44*, 67−72.
(20) Duffus, C. M.; Rosie, R. Some enzyme activities associated with the chlorophyll containing layers of the immature barley pericarp. *Planta* **1973**, *114*, 219−226.
(21) Tottman, D. R.; Makepeace, R. J. An explanation of the decimal code for the growth stages of cereals, with illustrations. *Ann. Appl. Biol.* **1979**, *93*, 221−234.
(22) Debeire-Gosselin, M.; Loonis, M.; Samain, E.; Debeire, P. Purification and properties of 22 kDa endoxylanase excreted by a new strain of thermophilic *Bacillus*. In *Xylans and Xylanases*; Visser, J., Beldman, G., Kusters-van Someren, M. A., Voragen, A. G. J., Eds.; Elsevier Science Publishers: Amsterdam, The Netherlands, 1992; pp 463−466.
(23) Kidby, D. K.; Davidson, D. J. A. Convenient ferricyanide estimation of reducing sugars in the nanomole range. *Anal. Biochem.* **1973**, *55*, 321−325.
(24) Benamrouche-Stitou, S. Biochimie et histologie de la dégradation enzymatique du son de blé par une endoxylanase. Ph.D. Dissertation, Université Reims Champagne-Ardenne, France, 2002.
(25) Verdeal, K.; Lorenz, K. Alkylresorcinols in wheat, rye, and triticale. *Cereal Chem.* **1977**, *54*, 475−483.
(26) Hamm, M.; Debeire, P.; Monties, B.; Chabbert, B. Changes in the cell wall network during the thermal dehydration of alfalfa stems. *J. Agric. Food Chem.* **2002**, *50*, 1897−1903.
(27) Zeier, J.; Schreiber, L. Comparative investigation of primary and tertiary endodermal cell walls isolated from the roots of five monocotyledoneous species: chemical composition in relation to fine structure. *Planta* **1998**, *206*, 349−361.
(28) Riederer, M.; Schönherr, J. Quantitative gas chromatographic analysis of methyl esters of hydroxy acids derived from plant cutin. *J. Chromatogr.* **1986**, *360*, 151−161.
(29) Kolattukudy, P. Biopolyester membranes of plants: cutin and suberin. *Science* **1980**, *208*, 990−999.
(30) MacMasters, M. M.; Hinton, J. J. C.; Bradbury, D. Microscopic structure and composition of the wheat kernel. In *Wheat Chemistry and Technology*; Pomeranz, Y., Eds.; Washington State University: Pullman, WA, 1978; pp 51−113.
(31) Briarty, L. G.; Hugues, C. E.; Evers, A. D. The developing endosperm of wheat. A stereological analysis. *Ann. Bot.* **1979**, *44*, 641−658.
(32) Harlan, H. V. Daily development of kernels of hannchen barley from flowering to maturity at Aberdeen, Idaho. *J. Agric. Res.* **1920**, *9*, 393−430.
(33) Morrisson, I. N.; Kuo, J.; O'Brien, T. P. Histochemistry and fine structure of developing wheat aleurone cells. *Planta* **1975**, *123*, 105−116.
(34) Hengtrakul, P.; Lorenz, K.; Mathias, M. Alkylresorcinol homologs in cereals grains. *J. Food Compos. Anal.* **1991**, *4*, 52−57.
(35) McCallum, J. A.; Walker, J. R. L. Phenolic biosynthesis during grain development in wheat (*Triticum aestivum* L.) III. Changes in hydroxycinnamic acids during grain development. *J. Cereal Sci.* **1991**, *13*, 161−172.
(36) Régnier, T.; Macheix, J. J. Changes in wall-bound phenolic acids, phenylalanine and tyrosine ammonia-lyases, and peroxidases in developing durum wheat grains (*Triticum turgidum* L. var. durum). *J. Agric. Food Chem.* **1996**, *44*, 1727−1730.
(37) McKeehen, J. D.; Busch, R. H.; Fulcher, R. G. Evaluation of wheat (*Triticum aestivum* L.) phenolic acids during grain development and their contribution to *Fusarium* resistance. *J. Agric. Food Chem.* **1999**, *47*, 1476−1482.
(38) Régnier, T. Les composés phénoliques du blé dur (*Triticum turgidum* L. var. durum): variations au cours du développement et de la maturation du grain. Relations avec l'apparition de la moucheture. Ph.D. Dissertation, Université Montpellier II, France, 1994.
(39) Ring, S. G.; Selvendran, R. R. Isolation and analysis of cell wall material from beeswing wheat bran (*Triticum aestivum*). *Phytochemistry* **1980**, *19*, 1723−1730.
(40) Ralph, J.; Quideau, S.; Grabber, J. H.; Hatfield, R. D. Identification and synthesis of new ferulic dehydrodymers present in grass cell walls. *J. Chem. Soc.* **1994**, *1*, 3485−3498.
(41) Garcia-Conesa, M. T.; Plumb, G. W.; Waldron, K. W.; Ralph, J.; Williamson, G. Ferulic acid dehydrodimers from wheat bran: isolation, purification and antioxidant properties of 8-O-4-diferulic acid. *Redox Rep.* **1997**, *3*, 319−323.
(42) Péyron, S.; Abecassis, J.; Autran, J. C.; Rouau, X. Influence of UV exposure on the phenolic acid content, the mechanical properties of the bran and the milling behaviour of durum wheat (*Triticum durum desf.*). *Cereal Chem.* **2002**, *79*, 726−731.
(43) Lapierre, C.; Monties, B.; Rolando, R. Thioacidolysis of poplar lignins: identification of monomeric syringyl products and characterization of guaiacyl-syringyl rich fractions. *Holzforschung* **1986**, *40*, 113−119.
(44) Antoine, C.; Peyron, S.; Mabille, F.; Lapierre, C.; Bouchet, B.; Abecassis, J.; Rouau, X. Individual contribution of grain outer layers and their cell wall structure to the mechanical properties of wheat bran. *J. Agric. Food Chem.* **2003**, *51*, 2026−2033.
(45) Terashima, N.; Fukushima, K.; He, L.-F.; Takabe, K. Comprehensive model of the lignified plant cell wall. In *Forage Cell Wall Structure and Digestibility*; Jung, H. G., Buxton, D. R., Hatfield, R. D., Ralph, J., Eds.; ASA, CSSA, SSSA: Madison, WI, 1993; pp 247−270.
(46) Fulcher, R. G.; O'Brien, T. P.; Lee, J. W. Studies on the aleurone layer, conventional and fluorescence microscopy of the cell wall with emphasis on phenol-carbohydrate complexes in wheat. *Aust. J. Biol. Sci.* **1972**, *25*, 23−34.

(47) Tervilä-Wilo, A.; Parkkonen, T.; Morgan, A.; Hopeakoski-Nurminen, M.; Poutanen, K.; Heikkinen, P.; Autio, K. *In vitro* digestion of wheat microstructure with xylanase and cellulase from *Trichoderma reesei*. *J. Cereal Sci.* **1996**, *24*, 215−225.
(48) Obel, N.; Porchia, A. C.; Scheller, H. V. Dynamic changes in cell wall polysaccharides during wheat seedling development. *Phytochemistry* **2002**, *60*, 603−610.
(49) Rhodes, D. I.; Stone, B. A. Proteins in walls of wheat aleurone cells. *J. Cereal Sci*. **2002**, *36*, 83−101.
(50) Rouau, X.; Cheynier, V.; Surget, A.; Gloux, D.; Barron, C.; Meudec, E.; Louis-Montero, J.; Criton, M. A dehydrotrimer of ferulic acid from maize bran. *Phytochemistry* **2003**, *63*, 899−903.
(51) Bunzel, M.; Ralph, J.; Kim, H.; Lu, F.; Ralph, S. A.; Marita, J. M.; Hatfield, R. D.; Steinhart, H. Sinapate dehydrodimers and sinapate-ferulate heterodimers in cereal dietary fiber. *J. Agric. Food Chem*. **2003**, *51*, 1427−1434.

Received for review March 23, 2004. Revised manuscript received August 6, 2004. Accepted August 30, 2004. This work was supported by a grant from the Région Champagne-Ardenne, France.

JF049529W